arXiv:1603.05546v1 [hep-ph] 17 Mar 2016

General considerations on the nature of $Z_b(10610)$ and $Z_b(10650)$ from their pole positions

Xian-Wei Kang [1],* Zhi-Hui Guo [2,3],† and J. A. Oller [1]‡
[1] *Departamento de Física, Universidad de Murcia, E-30071 Murcia, Spain*
[2] *Department of Physics, Hebei Normal University, Shijiazhuang 050024, Peoples Republic of China*
[3] *Helmholtz-Institut für Strahlen- und Kernphysik and Bethe Center for Theoretical Physics, Universität Bonn, D-53115 Bonn, Germany*

The nature of the bottomonium-like states $Z_b(10610)$ and $Z_b(10650)$ is studied by calculating the $B^{(*)}\overline{B}^*$ compositeness (X) in those resonances. We first consider uncoupled isovector S-wave scattering of $B^{(*)}\overline{B}^*$ within the framework of effective-range expansion (ERE). Expressions for the scattering length (a) and effective range (r) are derived exclusively in terms of the masses and widths of the two Z_b states. We then develop compositeness within ERE for the resonance case and deduce the expression $X = 1/\sqrt{2r/a-1}$, which is then applied to the systems of interest. Finally, the actual compositeness parameters are calculated in terms of resonance pole positions and their experimental branching ratios into $B^{(*)}\overline{B}^*$ by using the method of Ref. [1]. We find the values $X = 0.66 \pm 0.11$ and 0.51 ± 0.10 for the $Z_b(10610)$ and $Z_b(10650)$, respectively. We also compare the ERE with Breit-Wigner and Flatté parameterizations to discuss the applicability of the last two ones for near-threshold resonances with explicit examples.

I. INTRODUCTION

The discovery of exotic XYZ mesons, specially those with hidden charm or bottom quarks, opens a new era in hadron physics spectroscopy. Since the observation of $X(3872)$ [2], more than twenty XYZ mesons are observed by several experimental collaborations in last decade [3], for recent reviews see Refs. [4–6]. The conventional quark potential model, which is successful in describing the heavy quarkonium below the open heavy-flavor threshold, typically cannot well accommodate these XYZ states. Interestingly many of these exotic states share the common feature of lying nearby the thresholds of pairs of open charm/bottom mesons. In this respect, the effective range expansion (ERE) approach could provide a proper framework to study the physics in the vicinity of thresholds [7, 8].

Amongst the many observed XYZ mesons, we focus on the two bottomonium-like states $Z_b(10610)(Z_b)$ and $Z_b(10650)(Z_b')$ in the present work. They were measured by Belle Collaboration in the invariant mass spectra of $\pi^\pm\Upsilon(nS)$ $(n = 1, 2, 3)$ and $\pi^\pm h_b(mP)$ $(m = 1, 2)$, through the $\Upsilon(5S)$ decays with an additional charged pion [9]. All these five channels yield consistent values for the mass and width of the resonances [9], which are (in units of MeV)

$$\begin{aligned} M_{Z_b} &= 10607.2 \pm 2.0\,, \Gamma_{Z_b} = 18.4 \pm 2.4\,, \\ M_{Z_b'} &= 10652.2 \pm 1.5\,, \Gamma_{Z_b'} = 11.5 \pm 2.2\,. \end{aligned} \tag{1}$$

Later on, the two Z_b states were also confirmed in the $\Upsilon(5S) \to [B\overline{B}^* + c.c.]\pi$ and $B^*\overline{B}^*\pi$ channels [10]. Due to the noticeable feature that Z_b and Z_b' are charged bottomonium-like states, they can not be conventional heavy quarkonium. The neutral state $Z_b^0(10610)$ was also observed in $\Upsilon(5S) \to \Upsilon(nS)\pi^0\pi^0$ [11] with mass and width compatible with Eq. (1). The observed $Z_b^{(\prime)}$ have quantum numbers $I^G(J^P) = 1^+(1^+)$ [9, 12], so that their electrically neutral isotopic states ($I_3 = 0$) should have $J^{PC} = 1^{+-}$. Regarding this observation, the shorthand notation $B\overline{B}^*$ actually indicates the $G = +1$ combination $B\overline{B}^* - \overline{B}B^*$.

These exciting experimental observations have strongly intrigued theorists [4–6], and the properties of the $Z_b^{(\prime)}$ have been investigated in various theoretical approaches with the main aim of unveiling their nature. There are also proposals that the two Z_b resonances represent kinematical effects at thresholds, e.g. Refs. [13, 14] and [15]. The former two references interpret them as cusp effects, while the latter one advocates the energetic initial-single-pion emission mechanism to explain the experimental peak structures. However, Ref. [16] argues that such interpretations are not consistent. This reference shows that in order to produce peaks as pronounced and narrow as observed in experiment, nonperturbative interactions among the heavy mesons are necessary, which also give rise to the emergence of a nearby pole. Reference [16] also stresses the importance of measuring the transition of the near-threshold structure to the associated continuum channel (this is measured for the $Z_b^{(\prime)}$ in Ref. [10]) to properly check the assumption about a purely kinematic origin of near-threshold enhancements.

Several dynamical explanations have been proposed to study these resonances, including mesonic molecular states [17–28], compact tetraquark [29, 30], quark-gluon hybrid [30], hadro-quarkonium [31, 32], etc (see Refs. [4–6] for a more complete account of theoretical methods and related works). Typically the different models are

* xianwei.kang@um.es
† zhguo@mail.hebtu.edu.cn
‡ oller@um.es

characterized by assuming different constituents inside Z_b and Z_b' resonances. In the molecular picture the $Z_b^{(\prime)}$ contain pairs of heavy-light mesons (color-singlet clusters) that largely do not overlap within the molecule and keep basically their identities with small virtual three-momenta involved in the making up of the state [17–28]. On the contrary, more tightly packed states where the heavy and light quarks overlap would be generic multiquark states. For instance, two colored diquark-antidiquark clusters are assumed to be the dominant components in Ref. [29]. The quark-gluon hybrid approach advocates that the heavy quark-antiquark pair is embedded in the gluon and light-quark fields [30]. In the hadro-quarkonium model, the Z_b states are described as systems with a compact color-singlet heavy-quarkonium core surrounded by light hadronic fields extending over larger distances [31]. Tetraquark and open-heavy meson molecule pictures were also examined within QCD sum rules [33–37] and chiral quark models [22, 38]. Of course, it is possible that the observed $Z_b^{(\prime)}$ states could be an admixture of several proposed mechanisms.

In the present work we do not study any of the previous models in further detail, but focus on the energy regions in the vicinity of the $B\overline{B}^*$ and $B^*\overline{B}^*$ thresholds. We proceed in terms of general considerations from scattering theory, and no specific dynamics will be assumed. First we employ the ERE and later the method derived in Ref. [1]. Due to the fact that the central values of the masses of Z_b and Z_b' are only around 2–3 MeV above the $B\overline{B}^*$ and $B^*\overline{B}^*$ thresholds, respectively, we study the elastic isovector S-wave $B^{(*)}\overline{B}^*$ scattering that has the same quantum numbers as the resonances. We employ the uncoupled ERE for such aim up to the resonance pole positions. However, the nominal $B^{(*)}\overline{B}^*$ three-momentum at the pole position is around m_π (with m_π the pion mass), which is beyond the strict radius of convergence of the ERE, that cannot exceed the one-pion exchange branch point at momentum $k = im_\pi/2$. Nevertheless, there are serious indications that pion exchanges are perturbative for the $I^G(J^P) = 1^+(1^+)$ $B^{(*)}\overline{B}^*$ scattering in the low-energy region near threshold. In this respect, we have the estimates of Ref. [39], based on power counting in effective field theory, which establish that the iteration of pion exchanges is suppressed by a large expansion scale Λ, with $\Lambda \gg m_\pi$. This strong suppression confirms the observation of Ref. [26] that the exchange of light $q\bar{q}$ is Okubo-Zweig-Izuka (OZI) suppressed for the isovector $B^{(*)}\overline{B}^*$ scattering, a suppression that is seen in specific calculations too [15, 26, 40]. The same power counting study of Ref. [39] establishes that coupled-channel effects should be suppressed as well, at least a next-to-leading effect. This is further reinforced by the experimental measurement of the large branching ratios (Br) of $Z_b^{(\prime)}$ into $B^{(*)}\overline{B}^*$ [10].

As a result, the ERE study of the uncoupled isovector S-wave $B^{(*)}\overline{B}^*$ scattering seems to be a realistic first approximation to the study of the $Z_b^{(\prime)}$ resonances. Real values for scattering length (a) and effective range (r) are then required and we fix them by reproducing the corresponding pole positions, with the masses and widths given in Eq. (1).[1] Negative values for a and r are found between -1 and -2 fm. These natural values for the ERE parameters indicate that the generation of the $Z_b^{(\prime)}$ resonances does not require of any fine tuning, contrarily to e.g. S-wave nucleon-nucleon scattering and the deuteron or $\pi\Sigma_c$ scattering and the $\Lambda_c(2595)^+$ resonance [42, 43]. We also derive a general interpretation of compositeness (X) for resonances in ERE that is applicable as long as the resonance mass is above the corresponding threshold. If this condition is satisfied we find that $X = 1/\sqrt{2r/a - 1}$, plus contributions that would stem from higher orders in the ERE expansion. Based on this discussion we derive the scaling with the heavy-quark mass for the mass and width of a resonance whose composition is saturated by the two-heavy-particle component. This occurs when the resonance width is much larger than the difference between the resonance mass and the nearest threshold, a pattern that is approximately realized in many XYZ resonances (including the $Z_b^{(\prime)}$ resonances). Two simple potentials that can reproduce the values for a and r are discussed too. One of them contains only purely local interactions and the other is an attractive square-well potential. Through the compositeness analysis, one can infer the inner structures of the two Z_b states and we find that in the ERE case both resonances are dominated by the $B^{(*)}\overline{B}^*$ component, 76% (Z_b) and 68% (Z_b'), with an error of around 10%.

In the last part of the work, we make use of the method of Ref. [1] that is based on the expressions for the compositeness of a resonance (with mass higher than the lightest threshold) and its width (including effects from the mass distribution of the resonance due to its finite width). Its applicability does not depend on the strength of nearby branch points from crossed-channel dynamics nor on the presence of other channels.[2] Under the assumption that the partial decay widths of the $Z_b^{(\prime)}$ resonances into $B^{(*)}\overline{B}^*$ saturate the total widths we then reproduce the results of the ERE study. However, we can use this other method to derive the actual compositeness coefficients by taking into account the experimentally measured branching ratios of the $Z_b^{(\prime)}$ into $B^{(*)}\overline{B}^*$ decay channels by the Belle Collaboration [10]. We then find $X = 66\%$ (Z_b) and 51% (Z_b'), with around a 10% of error, for the $B\overline{B}^*$ and $B^*\overline{B}^*$ weights, respectively.

Notice that in this work the compositeness coefficients are purely determined by the masses and widths of $Z_b^{(\prime)}$ resonances. In this respect it is clearly different from

[1] Note that, in coupled channel scattering with missing channels the parameters in the ERE could be complex. For example, we refer to the analysis of the $p\bar{p}$ and $n\bar{n}$ in Ref. [41].

[2] As long as the assumed Lorentzian mass distribution for the resonance is not strongly distorted.

the procedure of Ref. [44], where the authors perform a combined analysis of data from the decays $\Upsilon(5S) \to h_b(1P,2P)\pi^+\pi^-$ and $\Upsilon(5S) \to B^{(*)}\overline{B}^*\pi$ in effective field theory from where they analyze the $B^{(*)}\overline{B}^*$ compositeness of $Z_b^{(\prime)}$, with values compatible with ours.

Finally, taking into account that the applicability of the ERE is not affected by the $B^{(*)}\overline{B}^*$ threshold, while this is the case for both Breit-Wigner and Flatté parameterizations, we then compare the amplitude squared from ERE with these other functions. In this way, we can gain some insight into the appropriateness of Breit-Wigner parameterizations to study the $Z_b^{(\prime)}$, as done by the Belle Collaboration [9–11]. We obtain that there is a marked cusp effect below threshold that can be well reproduced by a Flatté parameterization, but the Breit-Wigner function accurately reproduces $|t(E)|^2$ for $E > M_{\rm th}$ (including the maximum of the amplitude squared which fixes the resonance mass). As a result, we conclude that to apply Breit-Wigner functions to study the $Z_b^{(\prime)}$ is not unrealistic, at least as a first approach. Of course, sounder parameterizations are clearly required to improve accuracy. We also offer a variant of the Flatté parameterization that exactly reproduces the amplitude squared calculated from the ERE.

The article is organized as follows. After this Introduction we develop the ERE study of uncoupled isovector S-wave $B^{(*)}\overline{B}^*$ scattering around threshold in Sec. II, where the resulting values for a, r and the residues of the partial-wave amplitudes at the resonance pole positions are calculated. There we also adapt to nonrelativistic kinematics the calculation of compositeness X in Ref. [45] and derive an algebraic expression in terms of resonance mass and widths, Sec. II A. These results are then applied to the $Z_b^{(\prime)}$ resonances. In Sec. II B we consider the limit $X \to 1$ and the evolution of the pole position with the heavy quark mass. Section II C discusses two potentials that reproduce the values of a and r found for the $1^+(1^+)$ S-wave $B^{(*)}\overline{B}^*$ scattering. In Sec. III we apply the method of Ref. [1] and calculate the final compositeness coefficients in $B^{(*)}\overline{B}^*$ of $Z_b^{(\prime)}$ by taking into account their experimental branching ratios. Section IV contains a discussion about the question of applicability of Breit-Wigner and Flatté parameterizations to fit data in the study of these resonances. A summary of the results and conclusions are given in Sec. V .

II. EFFECTIVE RANGE STUDY

As explained in the Introduction we consider first the study of the uncoupled isovector S-wave $B^{(*)}\overline{B}^*$ scattering around threshold, that has the same quantum number as the $Z_b^{(\prime)}$ resonances. At first glance, the interest in this partial wave seems justified since the masses of $Z_b^{(\prime)}$ resonances are almost on top of the thresholds of $B^{(*)}\overline{B}^*$. Nonetheless, the nominal three-momenta of these particles in the pole positions corresponding to the resonances have a modulus of around m_π, so that a closer look is needed to justify the use of the ERE for the study of the resonances $Z_b^{(\prime)}$. Indeed the one-pion branch point is located at $k = im_\pi/2$ and then, strictly, the radius of convergence of the ERE is smaller than the distance to the resonance pole positions. At this stage, we make use of advances in the literature where it is shown that pion exchanges in the isovector $B^{(*)}\overline{B}^*$ scattering are expected to be clearly perturbative, since their iteration is suppressed by a large scale $\Lambda \gg m_\pi$ [39]. This outcome is based on derivations from power counting in chiral effective field theory [39, 46, 47]. This power counting establishes that coupled-channel effects are suppressed too, at least up to next-to-leading order. On the other hand, we also have the interesting observation of Ref. [26] which found that one light $q\bar{q}$-meson exchanges violate the OZI rule and are suppressed, while stressing the role of heavy-vector exchanges (that would correspond to contact interactions at low energy). Similar results were also obtained in previous studies in the charmonium sector [20, 48]. Then, we consider that for studying the $Z_b^{(\prime)}$ the use of the ERE up to their pole positions in the $1^+(1^{+-})$ $B^{(*)}\overline{B}^*$ uncoupled S-wave scattering seems a well suited first approximation.

The fact of disregarding coupled channel effects with other states that have different particle content to $B^{(*)}\overline{B}^*$, implies that the total widths of the $Z_b^{(\prime)}$ resonances must be saturated by their partial decay widths into $B^{(*)}\overline{B}^*$. This is a strong conclusion from the previous considerations that indeed can be checked experimentally since these branching ratios have been measured by Belle Collaboration in Ref. [10], where the following values are reported:

$$\begin{aligned} Br(Z_b(10610)^+ \to B\overline{B}^*) &= (86.0 \pm 3.6)\,\% \,, \\ Br(Z_b(10650)^+ \to B^*\overline{B}^*) &= (73.4 \pm 3.6)\,\% \,. \end{aligned} \tag{2}$$

We see that both Br's are rather large, which supports our way of proceeding.

The ERE gives rise to nonrelativistic $B^{(*)}\overline{B}^*$ partial-wave amplitudes that have exclusively right-hand cut or unitarity cut, without crossed-channel cuts. The general expression for a partial wave when crossed-channel cuts are absent is derived in Ref. [49] by making use of the N/D method [50], and it can be expressed as

$$t(E) = \left[\sum_i \frac{g_i}{E - M_{i,\rm CDD}} - ik \right]^{-1} . \tag{3}$$

Regarding the kinematical variables used in this equation, E is the center-of-mass (CM) energy of the system and k is the CM on-shell three-momentum. The nonrelativistic relation between E and k is valid for the present case and it reads

$$k = \sqrt{2\mu(E - M_{\rm th})} \,, \tag{4}$$

where $\mu = m_1 m_2/(m_1+m_2)$ is the reduced mass for the system with masses m_1 and m_2 and $M_{\rm th} = m_1 + m_2$ stands for the threshold.

The dynamical content of Eq. (3) is driven by the sum over the so-called Castillejo-Dalitz-Dyson (CDD) poles (each of them corresponds to a zero of $t(E)$ at $E = M_{i,\rm CDD}$), so that the $i_{\rm th}$ CDD pole is given in terms of its residue g_i and mass $M_{i,\rm CDD}$. The expansion in powers of k^2 of the CDD poles around $k = 0$ is equivalent to the ERE, but notice that this expansion would be valid until the position of the nearest CDD pole to threshold. Up to including $\mathcal{O}(k^2)$ in the expansion of $k \cot\delta_0$ (with δ_0 the isovector S-wave $B^{(*)}\overline{B}^*$ phase shifts) the ERE of the S-wave amplitude can be written as

$$t(E) = \frac{1}{-\frac{1}{a} + \frac{1}{2} r\, k^2 - i\, k} \ . \tag{5}$$

Here we have employed the same normalization as in Eq. (3), such that along the physical axis one has the unitarity condition

$$\mathrm{Im}\, t(E)^{-1} = -k \leq 0 \ . \tag{6}$$

However, the convergent range of the ERE would be severely restricted if any of the CDD poles in Eq. (3) had a mass very close to $M_{\rm th}$. This could be the case if the $Z_b^{(\prime)}$ had important components other than the $B^{(*)}\overline{B}^*$ ones, e.g. other heavier channels or corresponding to more elementary QCD degrees of freedom in terms of compact quark-gluon states [29–31, 37]. A distinctive feature of this situation can be recognized by considering the contribution of this CDD pole to a and r, which reads

$$\delta a = -\frac{M_{\rm th} - M_{i,\rm CDD}}{g_i} \ , \tag{7}$$

$$\delta r = -\frac{g_i}{\mu (M_{\rm th} - M_{i,\rm CDD})^2} \ . \tag{8}$$

As a result one should expect that if $M_{i,\rm CDD} \simeq M_{\rm th}$ a large absolute value of r would arise, because the denominator in Eq. (8) would involve the square of a small quantity (of the order of a kinetic energy, which also compensates for the appearance of the factor μ in this denominator). In this case the effective range r would be much larger than a standard value from potential scattering [7, 8], which typically would be similar to the natural range of strong interactions, $m_\pi^{-1} \sim \Lambda_{\rm QCD}^{-1} \sim 1$ fm, with $\Lambda_{\rm QCD}$ the typical QCD non-perturbative scale [3]. Then, the new small energy scale $|M_{i,\rm CDD} - M_{\rm th}|$ could totally spoil the application of the ERE analysis to the $Z_b^{(\prime)}$ states around the $B^{(*)}\overline{B}^*$ thresholds. We refer to Ref. [42] for a devoted discussion of the situation with $M_{\rm CDD} \simeq M_{\rm th}$ for the case of the resonance $\Lambda_c(2595)^+$ almost on top of the thresholds of the channels $\pi^0\Sigma_c^+$, $\pi^+\Sigma^0$ and $\pi^-\Sigma^{++}$.

Taking into account the previous warning, we apply first the ERE for $t(E)$ at the pole position $E = E_R$ of the resonance, with E_R given by

$$E_R = M_R - i\frac{\Gamma_R}{2} \ , \tag{9}$$

where M_R and Γ_R are its mass and width, in order.[3] We denote by $t_{II}(E)$ the partial-wave amplitude $t(E)$ in the 2nd Riemann sheet (RS), where the resonance pole lies. Its explicit form reads

$$t_{II}(E) = \frac{1}{-\frac{1}{a} + \frac{1}{2} r\, k^2 + i\, k} \ . \tag{10}$$

Notice the change of sign in front of k, compared to Eq. (5), with k given by Eq. (4) and calculated such that $\mathrm{Im}k > 0$ (1st RS). We denote by k_R the momentum at the resonance pole position,

$$k_R = \sqrt{2\mu(E_R - M_{\rm th})} \ , \tag{11}$$

and write it as

$$k_R = k_r + i\, k_i \ , \ k_i > 0 \ . \tag{12}$$

Let us derive a more explicit expression for k_R. For that we introduce the angle ϕ ($0 \leq \phi \leq \pi/4$) defined as

$$\tan 2\phi = \frac{\Gamma_R}{2|M_R - M_{\rm th}|} \ , \tag{13}$$

and in terms of it k_R reads

$$\text{i)}\ M_R - M_{\rm th} > 0 \ , \tag{14}$$

$$\begin{aligned} k_R =& \sqrt{2\mu|M_R - M_{\rm th} - i\frac{\Gamma_R}{2}|}\ \exp[i(\pi - \phi)] \\ =& \sqrt{2\mu|M_R - M_{\rm th} - i\frac{\Gamma_R}{2}|}\ (-\cos\phi + i\sin\phi) \ . \end{aligned}$$

$$\text{ii)}\ M_R - M_{\rm th} < 0 \ , \tag{15}$$

$$\begin{aligned} k_R =& \sqrt{2\mu|M_R - M_{\rm th} - i\frac{\Gamma_R}{2}|}\ \exp[i(\frac{\pi}{2} + \phi)] \\ =& \sqrt{2\mu|M_R - M_{\rm th} - i\frac{\Gamma_R}{2}|}\ (-\sin\phi + i\cos\phi) \ . \end{aligned}$$

The parameters a and r in the partial-wave amplitude $t(E)$ are fixed so as to reproduce the mass and width of the resonance, and from these values we can further discern whether there is an indication of a nearby CDD pole or just the opposite, i.e., a situation corresponding to a pure S-wave potential scattering problem. We find a and r by requiring that $t_{II}(E)^{-1} = 0$ at $E = E_R$, namely,

$$\begin{aligned} 0 =& -\frac{1}{a} + \frac{1}{2} r\, k_R^2 + i\, k_R \\ =& -\frac{1}{a} + \frac{1}{2} r\, (k_r^2 - k_i^2 + 2 i k_r k_i) + i k_r - k_i \ . \end{aligned} \tag{16}$$

[3] We have checked within the present ERE study that the resulting $t(E)$ above threshold is very well reproduced by a standard Breit-Wigner parameterization. So that the identification in Eq. (9) is consistent here.

Requiring the vanishing of both the real and imaginary parts of the previous equation, the following expressions result for $k_r \neq 0$

$$a = -\frac{2k_i}{|k_R|^2} \,, \tag{17}$$

$$r = -\frac{1}{k_i} \,. \tag{18}$$

Notice that given k_r and k_i one always finds a and r from Eqs. (17) and (18), respectively. For the opposite case, that is, once a and r are known, there is a resonance only if $a < 0$, $r < 0$ and $a/2 > r$, as it is clear from Eqs. (17,18). The case $k_r = 0$ corresponds to a virtual state, $M_R < M_{\rm th}$ and $\Gamma_R = 0$, and only one equation results then, $1/a + rk_i^2/2 + k_i = 0$.

Around the pole position we expand the denominator of $t_{II}(E)$ up to first order in $k - k_R$ and, by taking into account the resonance pole condition, cf. Eq. (16), the expression for $t_{II}(E)$ becomes

$$t_{II}(k) = \frac{1}{(rk_R + i)(k - k_R)} + \ldots = \frac{-k_i/k_r}{k - k_R} + \ldots \tag{19}$$

where we have used that $r = -1/k_i$, Eq. (18), and the ellipsis indicate higher order terms in the expansion in powers of $k - k_R$. From this equation we directly find the residue in the variable k,

$$\gamma_k^2 = -\frac{k_i}{k_r} > 0 \,. \tag{20}$$

Notice that $k_r < 0$, as it is clear from Eq. (14).

The residue of $t_{II}(E)$ in the standard Mandelstam variable $s = E^2$ is denoted by $-\gamma^2$,

$$t_{II}(E) \xrightarrow[E \to E_R]{} -\frac{\gamma^2}{s - E_R^2} \,. \tag{21}$$

Then, the relation between γ^2 and γ_k^2 follows straightforwardly

$$\gamma_k^2 = -\gamma^2 \left.\frac{dk}{ds}\right|_{k_R} = -\frac{\mu\gamma^2}{2E_R k_R} \,. \tag{22}$$

When solving $1/t_{II}(E_R) = 0$ for a and r, we also take into account the uncertainties in the pole positions of Z_b and Z_b' in Eq. (1). The numerical results are then given in Table I. In order to implement the error estimate, we discretize the pole mass and width at several points within around the one and a half σ region from the central values, so that a data grid results. For each of the points in the grid we calculate the corresponding a and r, cf. Eqs. (17,18), and the central values are given by the respective mean values and the errors by the square root of the variances. The procedure is of course stable by increasing the number of points in the grid and, e.g., convergence is already found when nine points in equal step for the mass and width are taken. The calculation of other quantities that stem from the knowledge of a and r will also follow this procedure.

	$Z_b(10610)$	$Z_b(10650)$
a (fm)	-1.03 ± 0.17	-1.18 ± 0.26
r (fm)	-1.49 ± 0.20	-2.03 ± 0.38
$X = \gamma_k^2$	0.75 ± 0.15	0.67 ± 0.16
g^2 (GeV^2)	362 ± 71	263 ± 63

TABLE I. From top to bottom and left to right, we give the scattering lengths (a) and effective ranges (r) of the $B\overline{B}^*$ (Z_b) and $B^{(*)}\overline{B}^*$ (Z_b') systems, in order. In the last two lines compositeness (X), which is equal to γ_k^2, and couplings squared g^2 for the $Z_b^{(\prime)}$ resonances are collected.

As it is clearly seen from Table I, the values for r correspond to the typical range of strong interactions, as they are of the order of $1/\Lambda_{\rm QCD}$. Because of this r behaves as expected for potential scattering [7, 8]. In particular, it excludes the possibility of having a nearby CDD pole around threshold because, as discussed above, it would give rise to large contributions in absolute value to r [42]. This fact, is also an indication that the $Z_b^{(\prime)}$ can be understood to large extent as $B^{(*)}\overline{B}^*$ resonances (in the case of uncoupled scattering).

A. Compositeness for a resonance within ERE

In order to further quantify the statement on the nature of the $Z_b^{(\prime)}$ as $B^{(*)}\overline{B}^*$ composite resonances we apply here the theory developed in Ref. [45], that allows a probabilistic interpretation of the compositeness relation [51–56] for those resonances such that $\sqrt{{\rm Re}E_R^2}$ is larger than the lightest threshold. We adapt the procedure of Ref. [45] to nonrelativistic kinematics, that is also the one employed in the ERE, cf. Eqs. (5) and (6).

We can follow analogous steps for the derivation of the criterion of applicability for the compositeness relation as done in Ref. [45] but now in the variable E instead of s. This change of variable is motivated by the fact that we are considering a nonrelativistic system. The Laurent series for $t_{II}(E)$ around $E = E_R$ in powers of $E - E_R$ has $|E_R - M_{\rm th}|$ as radius of convergence because of the branch point at threshold, cf. Eq. (4). As a result, as long as $M_R > M_{\rm th}$ this Laurent series always embraces a portion of the physical real axis and the probabilistic interpretation of X as the weight in the composition of the resonance then follows [45]. Notice that within the relativistic formalism of the latter reference the criterion for the applicability of this result is more restrictive because whenever $\sqrt{{\rm Re}E_R^2} > M_{\rm th}$ then $M_R > M_{\rm th}$ is fulfilled and no contradiction arises between our present criterion and that in Ref. [45]. At the practical level in our present application to the $Z_b^{(\prime)}$ resonances there is no difference

between both criteria because $\mathrm{Re}E_R^2 = M_R^2 - \frac{\Gamma_R^2}{4}$ and $(\Gamma_R/2M_R)^2 \sim 10^{-6}$.[4]

The nonrelativistic reduction of the unitarity loop function $G(E)$, with normalization

$$\mathrm{Im}\, G(E) = -k \ , \ k > 0 \tag{23}$$

according to the unitarity condition Eq. (6), is given by the integral representation ($\mathrm{Im}\, E \neq 0$)

$$G(E) = -\frac{E - M_{\rm th}}{\pi} \int_{M_{\rm th}}^{\infty} dE' \frac{\sqrt{2\mu(E' - M_{\rm th})}}{(E' - M_{\rm th})(E' - E)} + G(M_{\rm th}) \ . \tag{24}$$

One subtraction has been taken at threshold to end with a convergent integration, with the subtraction constant $G(M_{\rm th}) \in \mathbb{R}$. By rewriting $E' = M_{\rm th} + q^2/2\mu$ in Eq. (24) the latter becomes

$$G(E) = -\frac{k^2}{\pi} \int_0^{\infty} dq^2 \frac{1}{q(q^2 - k^2)} + G(M_{\rm th}) = -ik + G(M_{\rm th}) \ . \tag{25}$$

It need not be reiterated that $G(E)$ in the 1st RS is calculated with $\mathrm{Im}\, k \geq 0$, while in the 2nd RS $\mathrm{Im}\, k \leq 0$. In this latter case we denote the function $G(E)$ as $G_{II}(E)$. To avoid possible confusion with respect to the RS in which k is calculated we write our formulas such that k is calculated always in the 1st RS. In this from, $G_{II}(E)$ reads

$$G_{II}(E) = ik + G(M_{\rm th}) \ , \ \mathrm{Im}k > 0 \ . \tag{26}$$

From this equation we also obtain

$$\frac{dG_{II}(E)}{dk} = i \ . \tag{27}$$

Then, for $M_R \geq M_{\rm th}$ we have, according to procedure of Ref. [45], the following expression for the compositeness X,

$$X = \left| \gamma^2 \frac{dG(E_R)}{ds} \right| = \left| \gamma^2 \frac{dk}{ds} \frac{dG(E_R)}{dk} \right|^2 = |\gamma_k|^2 \ , \tag{28}$$

in virtue of the relation between the residues γ^2 and γ_k^2, cf. Eq. (22). Notice that X is independent of the subtraction constant because it disappears in $dG(E_R)/dk$.

Now, if we restrict ourselves to the ERE of $t_{II}(E)$ up to including $\mathcal{O}(k^2)$, Eq. (10), the residue γ_k^2 is given by Eq. (20), and then X reads

$$X = -\frac{k_i}{k_r} = \tan\phi \leq 1 \ , \tag{29}$$

because $\phi \in [0, \pi/4]$, cf. Eq. (13). According to Eqs. (14) and (15), the upper bound in the previous equation holds for $M_R \geq M_{\rm th}$, which shows the importance of fulfilling the criterion for compositeness so as to ascribe this meaning to X. Furthermore, the condition $M_R \geq M_{\rm th}$ deduced in the nonrelativistic discussion also provides a concrete example of the method of Ref. [45]. The elementariness Z is defined as

$$Z = 1 - X \ , \tag{30}$$

and $0 \leq Z \leq 1$ because of Eq. (29). We can also express X directly in terms of the observable quantities a and r since

$$X = -\frac{k_i}{k_r} = \left(\frac{2r}{a} - 1 \right)^{-\frac{1}{2}} \ , \tag{31}$$

as follows from Eqs. (17) and (18).

The saturation of the equality $X = 1$ occurs only for $M_R = M_{\rm th}$ and $\Gamma_R \neq 0$ ($\phi = \pi/4$) or, in other terms, when $a = r$, according to Eq. (31). In our present study this limit situation would correspond to $Z_b^{(\prime)}$ resonances composed purely of two heavy mesons.

Substituting Eq. (13) into Eq. (29) and performing the expansion in powers of $(M_R - M_{\rm th})/\Gamma_R$, another appealing way to express X is

$$X = -\frac{2(M_R - M_{\rm th})}{\Gamma_R} + \sqrt{1 + \left[\frac{2(M_R - M_{\rm th})}{\Gamma_R} \right]^2} = 1 - \frac{2(M_R - M_{\rm th})}{\Gamma_R} + 2 \left[\frac{(M_R - M_{\rm th})}{\Gamma_R} \right]^2 + \cdots \ , \tag{32}$$

where only the first three terms in the expansion are kept in the last line. This expression is explicitly given in terms of mass and width of the resonance, while in Refs. [51–56] the coupling strengths are usually needed to obtain X.

The experimental values of M_R for the $Z_b^{(\prime)}$ resonances fulfill the compositeness criterion $M_R \geq M_{\rm th}$, namely,

$$M_{Z_b^+} - \left[M_{B^+} + M_{\overline{B}^{*0}} \right] = (3.1 \pm 2.0) \ \mathrm{MeV}, \quad M_{Z_b'^+} - \left[M_{B^{*+}} + M_{\overline{B}^{*0}} \right] = (2.7 \pm 1.6) \ \mathrm{MeV}, \tag{33}$$

where we have employed the latest values for the masses from the PDG [3, 9]. Thus, we can calculate the compositeness coefficient X from Eq. (29) within the present ERE of uncoupled isovector S-wave $B^{(*)}\overline{B}^*$ scattering and the values are given in the 4th row of Table I. The approximated expression in the last line of Eq. (32) leads to $X = 0.73 \pm 0.15$ for Z_b and 0.66 ± 0.15 for Z_b', which are in good agreement with the exact numbers in Table I. These results indicate a large and dominant component of $B^{(*)}\overline{B}^*$ for the resonances $Z_b^{(\prime)}$, though still other components are not negligible. A sharper value of X would require to improve the precision in the experimental determination of the mass and width of the resonance.

[4] For the compositeness criterion an expansion in energy not in momentum is employed because one is extrapolating in the resonance mass from the narrow resonance case to the inner complex plane.

B. Scaling of the width in heavy-meson composite resonances

For the $Z_b^{(\prime)}$ resonances one has that the (small) width is significantly larger than the difference between the resonance mass and the close $B^{(*)}\overline{B}^*$ heavy-meson threshold, cf. Eqs. (1) and (33). This is also a typical situation for many of the reported XYZ resonances. If this is the case and the ERE can be applied, as argued above this is expected to be a good (first) approximation for the $Z_b^{(\prime)}$, one can derive a simple way a scaling law for the width of the resonance. Let us recall that according to the discussion in Sec. II A the limit $2(M_R - M_{\rm th})/\Gamma_R \to 0$ correspond to a resonance made purely by the two heavy-mesons ($X \to 1$).

The resonant momentum k_R in the limit $\Gamma_R/2 \gg |M_R - M_{\rm th}|$ becomes in good approximation,

$$k_R \approx \sqrt{-i\mu\Gamma_R} = -e^{-i\frac{\pi}{4}}\sqrt{\mu\Gamma_R}\ , \tag{34}$$

as follows by applying Eq. (14) with $\phi = \pi/4$ and neglecting $|M_R - M_{\rm th}|$ in front of $\Gamma_R/2$. As a result

$$-k_r \approx k_i \approx \sqrt{\frac{\mu\Gamma_R}{2}}\ . \tag{35}$$

This result implies because of Eq. (18) that

$$r \approx -\sqrt{\frac{2}{\mu\Gamma_R}}\ . \tag{36}$$

We further require that r has a natural size for strong interactions, so that a CDD pole near threshold, which would give rise to a large contribution to r for $M_{\rm CDD} \to M_{\rm th}$, cf. Eq. (7), is excluded. Then, with $r \sim -\frac{1}{\Lambda_{\rm QCD}}$ we find from Eq. (36) an order of magnitude estimate for Γ_R,

$$\Gamma_R \sim \frac{2\Lambda_{\rm QCD}^2}{\mu} \tag{37}$$

Since we assume that $\Gamma_R/2 \gg |M_R - M_{\rm th}|$ one has the consistency requirement that

$$\frac{\Lambda_{\rm QCD}^2}{\mu} \gg |M_R - M_{\rm th}|. \tag{38}$$

Eqs. (37) and (38) imply that as the heavy-quark mass increases the resonances composed mainly by the heavy-flavor mesons should become narrower and basically sit on top of threshold in the energy plane. However, let us notice that k_R is stable because of the product of μ and Γ_R,

$$k_R \approx \sqrt{-i\mu\Gamma_R} \sim -e^{-i\frac{\pi}{4}}\sqrt{2}\Lambda_{QCD}\ . \tag{39}$$

The estimate of the width for the $B^{(*)}\overline{B}^*$ systems from Eq. (37) gives $\Gamma_R \sim 30$ MeV. Here we have taken $\Lambda_{\rm QCD} \simeq 200$ MeV, because the momentum transfer is small and this corresponds to the first few low-mass quark flavors. The estimated value for Γ_R agrees with the experimental widths of the $Z_b^{(\prime)}$, Eq. (1), within a factor of around 2. The consistency check of Eq. (38) is well fulfilled because the differences between resonance masses and thresholds, cf. Eq. (33), are considerably smaller than $\Lambda_{\rm QCD}^2/\mu \sim 15$ MeV.

C. Two simple models as examples

Here we present two potentials that reproduce exactly the values of a and r deduced above from the ERE application to the study of the pole positions of the $Z_b^{(\prime)}$ resonances.

As a first example, we consider a pure contact theory with an S-wave potential of the form

$$v(p,k) = C_0 + C_2(p^2 + k^2)\ , \tag{40}$$

with p and k three-momenta. In terms of this potential one can reproduce any negative values for a and r. This can be explicitly shown by solving the corresponding Lippmann-Schwinger equation

$$t(p,k;E) = v(p,k) + \frac{2}{\pi}\int_0^\infty dq \frac{q^2 v(p,q)t(q,k;E)}{q^2 - k^2 - i0^+}\ , \tag{41}$$

such that $E = k^2/2\mu$ and the on-shell T-matrix element, $t(k,k;k^2/2\mu)$ corresponds to $t(E)$, already introduced. One can easily solve Eq. (41) by proposing a solution of the form

$$t(p,k;k^2/2\mu) = t_0(k) + t_2(k)(k^2 + p^2)\ . \tag{42}$$

The integrations in the variable q^2 can be done with a three-momentum cut-off Λ. For a given Λ one then solves C_0 and C_2 such that the values for a and r are reproduced. This makes that both C_0 and C_2 become function of Λ. Real solutions $C_0(\Lambda)$ and $C_2(\Lambda)$ exist whenever $r < 0$, e.g. we have for $C_2(\Lambda)$,

$$C_2\Lambda^3 = -\frac{3\pi}{2}\left\{1 \pm \frac{\sqrt{3}(\pi - 2\alpha)}{\sqrt{3(2\alpha - \pi)^2 + 4\alpha^2 - \alpha^2\rho\pi}}\right\}\ , \tag{43}$$

where $\alpha = a\Lambda$ and $\rho = r\Lambda$. The crucial property to end with real counterterms (as required for the potential in Eq. (40) to be Hermitian) is to demand that the radicand in the previous equation be positive,

$$3(2\alpha - \pi)^2 + 4\alpha^2 - \alpha^2\rho\pi \geq 0\ , \tag{44}$$

which is always the case if $r < 0$ ($\rho < 0$). In the limit $\Lambda \to \infty$ one obtains exactly the ERE approximation for $t(E)$ of Eq. (5),

$$t(E) = \frac{1}{-\frac{1}{a} + \frac{1}{2}rk^2 - ik} + \mathcal{O}(\Lambda^{-1})\ . \tag{45}$$

Ref. [57] finds that a renormalized effective field theory with only contact interactions gives rise to an ERE (although the reverse is not always true [58], cf. restriction in Eq. (44)). Thus, a contact interaction theory with two couplings can exactly reproduce the results obtained before in the ERE study, for which a and r are negative.

The second example corresponds to a simple attractive square-well potential of radius R ,

$$v(r) = -V_0\theta(R-r) \ , \tag{46}$$

with $V_0 > 0$. The S-wave amplitude can be easily found, e.g. by solving the corresponding Schrödinger equation

$$\left\{\frac{d^2}{dr^2} + 2\mu V_0\theta(R-r) + k^2\right\} u(r) = 0 \ , \tag{47}$$

with $u(r)$ the reduced wave function. This is explicitly solved e.g. in Ref. [59]. The resulting S matrix is

$$\begin{aligned} S(E) =& e^{2i\delta_0(E)} \\ =& e^{-2ikR}\frac{e^{ik'R}(k+k') + e^{-ik'R}(k'-k)}{e^{-ik'R}(k+k') + e^{ik'R}(k'-k)} \ , \end{aligned} \tag{48}$$

where

$$k' = \sqrt{k^2 + 2\mu V_0} \ . \tag{49}$$

The ERE is obtained from the expansion in powers of k^2 of

$$k\cot\delta_0 = k\cot\left[-kR + \arctan\left\{\frac{k}{k'}\tan\left(k'R\right)\right\}\right] \ . \tag{50}$$

The corresponding expressions for a and r are

$$a = R\left(1 - \frac{\tan\gamma}{\gamma}\right) \ , \tag{51}$$

$$r = R\left(1 - \frac{1}{\gamma^2 x} - \frac{1}{3x^2}\right) \ , \tag{52}$$

with the dimensionless variables

$$\begin{aligned} \gamma =& R\sqrt{2\mu V_0} \ , \\ x =& a/R \ . \end{aligned} \tag{53}$$

If we consider the application of this toy model to the isovector S-wave $B^{(*)}\overline{B}^*$ scattering one expects that the value of $\gamma^2 \gg 1$ by taking the simple dimensional estimates $R \simeq 1/\Lambda_{QCD}$ and $V_0 \simeq \Lambda_{QCD}$, together with $\mu \simeq M_B/2 \simeq 2.6$ GeV, where M_B is the mass of the B meson.[5] Then

$$\gamma^2 \sim \frac{M_B}{\Lambda_{\rm QCD}} \sim 30 \ . \tag{54}$$

As a result, in order to end with a negative value for a from Eq. (51) (so that $\tan\gamma/\gamma > 1$), it is necessary that

$$\gamma \to (n + \frac{1}{2})\pi \ , \tag{55}$$

with $n \sim 1$, 2 to match the estimate in Eq. (54).

The parameter x has a well-defined limit for $\gamma^2 \to \infty$. To obtain this conclusion we first notice that x can be fixed by the ratio r/a, since it results from Eqs. (51,52) that

$$\frac{r}{a}3x^3 - 3x^2 + \frac{3x}{\gamma^2} - 1 = 0 \ . \tag{56}$$

This equation for $\gamma^2 \gg 1$ becomes independent of this parameter, and one has the following asymptotic equation

$$\frac{r}{a}3x_\infty^3 - 3x_\infty^2 - 1 = 0 \ . \tag{57}$$

Next, it is easy to show that the difference between the actual value of γ and $(n+\frac{1}{2})\pi$ should scale as $1/\sqrt{\mu}$. Calling this difference ε we would have from Eq. (51) that

$$\frac{\tan\gamma}{\gamma} = 1 - x \to 1 - x_\infty \ , \tag{58}$$

which is a fixed number (around 1.5 by explicitly solving Eq. (57) with the values for a and r given in Table I.) Then,

$$\frac{\tan\gamma}{\gamma} = \frac{\tan\left[(n+1/2)\pi + \varepsilon\right]}{\gamma} \sim -\frac{1}{\varepsilon\gamma} = 1 - x_\infty \ . \tag{59}$$

In this way we conclude that

$$\varepsilon \sim \frac{1}{\gamma} \sim \left(\frac{\Lambda_{\rm QCD}}{\mu}\right)^{\frac{1}{2}} \ . \tag{60}$$

However, k_R corresponding to the resonance poles of $S(E)$ does not run with μ. This is clear if we consider the equation satisfied by k_R,

$$k_R^2 + \gamma^2\cos^2(k'_R R) = 0 \tag{61}$$

that results from Eq. (48) by requiring that $S(E_R)^{-1} = 0$. For large γ^2, with $\gamma_0^2 = [(n+1/2)\pi]^2$, Eq. (61) can be expressed as

$$k_R^2 + R^{-2}\mathcal{O}(1) = 0 \ , \tag{62}$$

where one has to notice that $k'_R R = \gamma_0\sqrt{1 + (k_R R/\gamma_0)^2 + (1+\varepsilon/\gamma_0)^2}$ and $\cos((n+1/2)\pi + \delta) = -(-1)^n\delta + \mathcal{O}(\delta^3)$.

Let us also mention that the limit $\gamma \to (n+1/2)\pi - 0^+$ implies $a = -\infty$ (for fixed n), which is a virtual state at threshold. This is the ending (never reached) point that continuously connects with the resonance case that we are discussing by extrapolating the resonance mass below threshold. The fact that k_R does not scale with μ

[5] The departure of the estimate $r \sim R$ (used in Sec. II B) from Eq. (52) with large γ would require $x \to 0$, which is far from our case since we have $x \sim -1$, cf. Table I. Indeed for $x = 0$ the ERE breaks down because then $k\cot\delta(0) = \infty$.

is an exemplification of the considerations that we already explored within the ERE and heavy quark limit in Sec. II B (for $X \to 1$), cf. Eq. (39).[6]

III. COMPOSITENESS AND WIDTH

It is clear that in the uncoupled ERE with *real* values of a and r the full widths of the $Z_b^{(\prime)}$ should correspond to the partial decay widths into the channels $B^{(*)}\overline{B}^*$. This is a bonus of the ERE approach employed here since in this way one does not need to apply a (heuristic) formula to reproduce the width of a resonance in terms of its coupling. This was e.g. the case in Ref. [1] to account for the $\chi_{c1}p$ width of $P_c(4450)$ (note the two-channel problem there, namely $J/\psi p$ and $\chi_{c1}p$). However, the method of Ref. [1] allows one to drop several assumptions inherent to the ERE study of the uncoupled isovector S-wave $B^{(*)}\overline{B}^*$ scattering performed in the previous section. This is convenient because then one does not need to assume the particle content for the involved states nor scattering in just one partial wave (several partial waves per channel could be possible). In addition, this method is rather insensitive to the issue of the strength of nearby branch points from crossed-particle exchanges.[7]

We start by extending the brief discussion given in Ref. [1], which establishes a rather clear picture for the width of the resonance in terms of $|\gamma|^2$ and the mass distribution induced by the finite width itself. On the one hand, we have the standard two-body decay formula [3] of a resonance into one channel in terms of its coupling squared. The corresponding equation in our normalization, Eq. (6), can be easily deduced by considering that $t(E)$ is saturated by the resonance contribution, $t(E) \to -\gamma^2/(s - s_R)$, and then requiring the fulfillment of the unitarity condition Eq. (6). This implies

$$k = M_R \Gamma_R(E)/\gamma^2 \ . \tag{63}$$

We then deduce the expression,

$$\Gamma^{(1)} = \frac{k(M_R)|\gamma^2|}{M_R} \ . \tag{64}$$

We take the modulus of the residue in Eq. (64) because it is generally a complex number, cf. Eq. (22). The decay width formula Eq. (64) should be valid for a narrow resonance when the distances between M_R and decay-channel thresholds are large in comparison with the resonance width (this latter condition is not satisfied by the $Z_b^{(\prime)}$ resonances.)

Another point worth stressing with respect to Eq. (64) is that this equation applies to the width of a resonance independently of its angular momentum because the unitarity requirement Eq. (6) is valid for any partial wave (not only for S-wave). The same can be said for the compositeness X of Eq. (28), that applies to any angular-momentum resonance, as it is clear from the analysis undergone in Ref. [45]. As a result, if a two-body particle decay channel appears in several partial waves for a given resonance (due to the mixing of orbital angular momentum and spin quantum numbers) the total decay width and compositeness of the resonance in such decay channel are given by Eqs. (64) and (28), but with $|\gamma^2|$ corresponding to the sum of the residues of all partial waves involved, $|\gamma^2| = \sum_i |\gamma_i^2|$.

The expression for $\Gamma^{(1)}$ in terms of γ_k^2 follows from Eq. (64) by taking into account the relationship between γ^2 and γ_k^2 given in Eq. (22). The result is

$$\Gamma^{(1)} = \frac{2\gamma_k^2}{\mu} k(M_R)|k_R| \ . \tag{65}$$

The more standard form of $\Gamma^{(1)}$, e.g. the one appearing in Ref. [3], implies to use the resonance coupling squared g^2, which in terms of the residue γ^2 corresponds to

$$g^2 = \left|\gamma^2 8\pi E_R\right| \simeq |\gamma^2| 8\pi M_R \ . \tag{66}$$

In the last step we have used that $M_R \gg \Gamma_R/2$ for the $Z_b^{(\prime)}$. In terms of g^2 Eq. (64) becomes

$$\Gamma^{(1)} = \frac{k(M_R) g^2}{8\pi M_R^2} \ . \tag{67}$$

On the other hand, we also have the more elaborated decay width formula [1, 61]

$$\Gamma^{(2)} = \frac{g^2}{16\pi^2} \int_{M_{\rm th}}^{+\infty} \frac{dW k(W)}{W^2} \frac{\Gamma_R}{(M_R - W)^2 + \Gamma_R^2/4} \tag{68}$$

$$= \frac{X|k_R| M_R^2}{\pi\mu} \int_{M_{\rm th}}^{+\infty} \frac{dW k(W)}{W^2} \frac{\Gamma_R}{(M_R - W)^2 + \Gamma_R^2/4} \tag{69}$$

where $k(W)$ is the three-momentum as a function of the total energy W, cf. Eq. (4). The latter variable is distributed around the resonance mass according to the Lorentzian mass distribution of mass M_R and width Γ_R. The last Eq. (69) results from Eq. (68) by taking into account the relationship between g^2 and γ_k^2, cf. Eqs. (22), (28) and (66).

We offer here a brief derivation of Eq. (68). For that we allow to vary the invariant mass W of the two-body

[6] Nevertheless, one has not to pursue too far the analogy with the spectroscopy of the square-well potential because this depends on higher-order shape parameters in the ERE, and then it is more sensitive to the finer details of the toy model. In this respect we notice that for $|k_R| < 1/R$ all the poles of $S(E)$ lie along the imaginary axis [57, 60], while the ERE for this potential is valid up to $|k| \lesssim 1.3/R$ ($r/a = 1$), as follows from the position of the closest zero of $t(E)$ at threshold. However, a and r parameterize the low-energy limit of the T-matrix and are sensitive to the global aspects of the potential, characterized by its strength and range.

[7] Nevertheless, it is assumed that a Lorentzian mass distribution with a constant coupling holds for the resonance, which could be affected by the presence of nearby and strong crossed-particle-exchange branch points.

decay channel according to a mass distribution $F(W)$ around the nominal resonance mass M_R and denote by $\mathcal{M}$ the corresponding resonance coupling/residue (which could also depend on W). In this way, instead of Eq. (67) we have now the more general expression

$$\Gamma = \int_{M_{\rm th}}^{+\infty} \frac{dW k(W)}{8\pi W^2} |\mathcal{M}|^2 F(M) \ , \tag{70}$$

where the lower limit of integration results because the two particles in the decay channels are the asymptotic ones.

For a narrow resonance one typically takes

$$F(M) = \delta(W - M_R) \ , \tag{71}$$

which, after being inserted in Eq. (70), leads to Eq. (67). When finite-width effects are considered a standard and simple option is to use for $F(W)$ a Lorentzian mass distribution,

$$\begin{aligned} F(W) =& \frac{1}{\pi} {\rm Im} \frac{1}{W - M_R - i\Gamma_R/2} \\ =& \frac{1}{2\pi} \frac{\Gamma_R}{(W-M_R)^2 + {\Gamma_R}^2/4} \end{aligned} \tag{72}$$

and then Eq. (68) results if additionally $|\mathcal{M}|^2 \to g^2$, so that any possible energy dependence is neglected. Indeed, Eq. (67) stems also from Eq. (68) in the limit of zero width, being the later much more adequate to take into account finite-width effects. For example, the mass of the $P_c(4450)$ [62] at its lower range within error bars lies indeed below the $\chi_{c1}p$ mass so that one cannot apply Eq. (67), since then k would become complex. This caveat is solved with the use of Eq. (68), and the error estimate of the calculated width can be performed rather straightforwardly from the experimental errors of the mass and width of $P_c(4450)$.

For the practical use of Eq. (68) we distinguish between integrating up to ∞ or up to $M_R + n\Gamma_R$, with n fixed such that $\Gamma^{(2)}$ coincides with the experimental value. Proceeding in this way is justified because the Lorentzian mass distribution has a long tail which gives rise to a slow convergence of the integration in Eq. (68). The resulting width from the integration up to ∞ is denoted by $\Gamma^{(2)}_>$ and the one up to $M_R + n\Gamma_R$ by $\Gamma^{(2)}_<$.

We first consider the value for g^2 corresponding to the ERE results (last row of Table I). In this case, consistency between ERE and the present method requires that the calculated width in terms of the coupling be the same as the experimental one (the one imposed in the ERE analysis of Sec. II). The numerical values of $\Gamma^{(1)}$, $\Gamma^{(2)}_>$ and $\Gamma^{(2)}_<$ are summarized in Table II. From the table, we see that these widths are compatible with the measured Γ_R in Eq. (1) within errors. The width $\Gamma^{(2)}_<$ reproduces exactly the experimental width with $n \simeq 8$, that will be used in the following whenever we employ Eq. (68) with a finite upper integration limit. Of course, $\Gamma^{(2)}_>$ is larger than $\Gamma^{(2)}_<$, as indicated by the subscripts, due to the larger integration region for a positive integrand in Eq. (68).

Γ (MeV)	$Z_b(10610)$	$Z_b(10650)$
$\Gamma^{(1)}$	14.9 ± 2.3	9.5 ± 2.1
$\Gamma^{(2)}_>$	21.9 ± 3.3	13.4 ± 2.8
$\Gamma^{(2)}_<$	18.5 ± 2.4	11.3 ± 2.1

TABLE II. Widths of the $Z_b^{(\prime)}$ obtained by using the coupling squared g^2 from the ERE, cf. Table I. For their calculation we have considered both $\Gamma^{(1)}$, Eq. (67), and $\Gamma^{(2)}$, (68). For the latter case the subscripts $>$ and $<$ refer to the integration regions employed in Eq. (68), $[M_{\rm th}, \infty)$ and $[M_{\rm th}, M_R + n\Gamma_R]$, $n = 8$, in order.

	$Z_b(10610)$	$Z_b(10650)$
$\Gamma = \Gamma_R$	$X = 0.76 \pm 0.12$	$X = 0.69 \pm 0.14$
$\Gamma = \Gamma_R \cdot {\rm Br}$	$X_{\rm ex} = 0.66 \pm 0.11$	$X_{\rm ex} = 0.51 \pm 0.10$

TABLE III. Compositeness coefficient X in the limit case of saturating the experimental total width $\Gamma = \Gamma_R$ (2nd row) and $X_{\rm ex}$ (last row), that takes into account the experimentally measured partial decay widths of $Z_b^{(\prime)}$ into $B^{(*)}\overline{B}^*$ [10].

Now, we follow the method of analysis of Ref. [1], that heavily relies in the expressions for the width, Eq. (68), and compositeness X, Eq. (28). As indicated at the beginning of this Section, we do not need to assume in this way that the $Z_b^{(\prime)}$ resonances stem from uncoupled isovector S-wave $B^{(*)}\overline{B}^*$ scattering, nor the applicability itself of the ERE up to the resonance pole positions, as done in the ERE study of Sec. II.

Firstly, we perform two consistency checks between the previous ERE study in Sec. II and the new one based on the approach of Ref. [1]. On the one hand, we take the same basic assumption as in the ERE, so that the only relevant open channel around the resonance energy region would be the $B\overline{B}^*$ ($B^*\overline{B}^*$) for the $Z_b(Z_b')$ resonance. As a result, we assume that $B^{(*)}\overline{B}^*$ saturate the experimental total decay widths of $Z_b^{(\prime)}$, namely, $\Gamma^{(2)} = \Gamma_R$. From this requirement we can calculate the value of X from Eq. (69), with the resulting expression

$$X = \frac{\mu\pi}{|k_R| M_R^2 \int_{M_{\rm th}}^{W_+} \frac{dW k(W)/W^2}{(M_R - W)^2 + {\Gamma_R}^2/4}} \ , \tag{73}$$

where $W_+ = M_{\rm th} + n\Gamma^{(2)}$, and $n = 8$ (as previously used to exactly reproduce the experimental width of the $Z_b^{(\prime)}$ in the last column of Table II). The calculated X is given in the 2nd row of Table III and perfectly agrees with the one found in the ERE study, cf. Table I. This consistency check would become a physical test of the

ERE applicability in the study of the $Z_b^{(\prime)}$ resonances if a and r were actually measured experimentally in near threshold $1^+(1^+)$ $B^{(*)}\overline{B}^*$ scattering.

For the second consistency check, we assume that the two-body states $B^{(*)}\overline{B}^*$ saturate the components of $Z_b^{(\prime)}$, i.e., $X \to 1$. This assumption also implies that the resonance should fully decay into $B^{(*)}\overline{B}^*$ because the coupling to any other open channel should tend to zero (otherwise X would depart from 1). In this case γ_k^2 takes its maximum possible value, $\gamma_k^2 = 1$. One can then deduce the value for the width of the resonance to $B^{(*)}\overline{B}^*$ under such circumstances by making use of Eq. (69) with $X = 1$ and Γ_R in the right-hand side replaced by $\Gamma^{(2)}$. The following implicit equation for $\Gamma^{(2)}$ results:

$$1 = \frac{|k(M_R - i\frac{\Gamma^{(2)}}{2})|M_R^2}{\pi\mu} \times \int_{M_{\rm th}}^{W_+} \frac{dW k(W)}{W^2} \frac{1}{(M_R - W)^2 + {\Gamma^{(2)}}^2/4} \ , \tag{74}$$

with W_+ evaluated with $n = 8$ as in Eq. (73). One then obtains that $\Gamma^{(2)}$ becomes huge (in practical terms ∞) around several hundreds of MeV. This is in agreement with Eq. (29) for X in the ERE, such that the limit $X \to 1$ with $M_R - M_{\rm th} \neq 0$ strictly requires that $\Gamma \to \infty$.

Importantly, the branching ratios for the partial decay widths of $Z_b^{(\prime)}$ into $B^{(*)}\overline{B}^*$ have been measured by Belle Collaboration in Ref. [10], cf. Eq. (2). Although these figures are large, the Br's are clearly less than 1, so that $\Gamma_R \neq \Gamma(Z_b^{(\prime)} \to B^{(*)}\overline{B}^*)$. In order to take care of this experimental fact and provide a more accurate determination of X one has to depart from the ERE study and use the method of Ref. [1]. The latter allows us to find the actual compositeness coefficient X (denoted by $X_{\rm ex}$) by making use of Eq. (69) with $\Gamma^{(2)} = \Gamma_R Br$. One then finds for $X_{\rm ex}$,

$$X_{\rm ex} = \frac{\pi\mu\, Br(Z_b^{(\prime)} \to B\overline{B}^*)}{|k_R| M_R^2 \int_{M_{\rm th}}^{W_+} \frac{dW k(W)}{W^2} \frac{1}{(M_R - W)^2 + \Gamma_R^2/4}} \ . \tag{75}$$

The results obtained with $W_+ = M_{\rm th} + 8\Gamma_R$ are shown in the last row of Table III, being almost identical to those that would result if we had used instead $\Gamma^{(1)}$ from Eq. (65) (as we have checked). The $B\overline{B}^*$ weight calculated within the Z_b is $(66 \pm 11)\%$, and the $B^*\overline{B}^*$ one for the Z_b' is $(51 \pm 10)\%$. We then conclude that the $B\overline{B}^*$ weight is dominant for the Z_b, while the $B^*\overline{B}^*$ component is around one half of the total composition of the Z_b'. As a result, other non $B^{(*)}\overline{B}^*$ components play a more important role for the latter, being appreciable for both resonances. This is also clear by comparing $X_{\rm ex}$ in Table III with the compositeness coefficient deduced in the ERE study, cf. 3rd row of Table I. For the Z_b state both calculations have similar central values while for the Z_b' they are more different, though still compatible within error bars. This latter fact also reflects the smaller branching ratio for the Z_b' in Eq. (2). We also mention that our results for $X_{\rm ex}$ are similar to those in Ref. [44], where X for each resonance is estimated to be around 60%.

IV. ERE VS. BREIT-WIGNER AND FLATTÉ PARAMETERIZATIONS

We now address the question about the applicability of Breit-Wigner functions in the experimental analyses of Refs. [9–11] for the $Z_b^{(\prime)}$ due to the closeness of the thresholds of the $B^{(*)}\overline{B}^*$ states, an issue stressed e.g. in Refs. [18, 63, 64]. The ERE is adequate to check whether a Breit-Wigner (or Flatté) function is appropriate since the applicability of ERE is not affected by the threshold singularity associated with the $B^{(*)}\overline{B}^*$. For definiteness let us take the central values of a and r in Table I for the Z_b (analogous conclusions would equally apply to the Z_b'). We are going to compare $|t(E)|^2$ calculated within the ERE, cf. Eq. (5), with i) a Breit-Wigner function of constant width, $bw(E)$,

$$bw(E) = |t(M_R)|^2 \frac{\Gamma_R^2/4}{(E - M_R)^2 + \Gamma_R^2/4} \tag{76}$$

and ii) with a Flatté parameterization [65], $ft(E)$,

$$ft(E) = \frac{f_0}{|E - M_R' + i\,\Gamma_R(E)/2|^2} \ . \tag{77}$$

Here $\Gamma_R(E)$ is the analytically-continued energy-dependent width that in the 1st RS along the real axis corresponds to, cf. Eq. (63),

$$\begin{aligned} \Gamma_R(E) &= \frac{2\gamma_k^2}{\mu} k(E)|k_R| \ , \ E \geq M_R \ , \\ &= i\frac{2\gamma_k^2}{\mu} |k(E) k_R| \ , \ E < M_R \ . \end{aligned} \tag{78}$$

In addition, M_R' is fixed such that the real part of the complex number in the denominator of Eq. (77) vanishes at the pole position $E = E_R$ (in the 2nd RS). This implies the equation

$$M_R' = M_R + \gamma_k^2 k_i |k_R|/\mu \ . \tag{79}$$

The normalization factors $|t(M_R)|^2$ in Eq. (76) and f_0 in Eq. (77) are fixed such that the maximum value of the Breit-Wigner and Flatté parameterizations coincides with the maximum of $|t(E)|^2$.

We perform this comparison in the top panel of Fig. 1 where the solid line corresponds to $|t(E)|^2$, the dashed curve to $bw(E)$ and the dash-dotted one to $ft(E)$. On the one hand, we see that $bw(E)$ lies on top of $|t(E)|^2$ above threshold, while below it they do not follow each other due to the cusp effect in $|t(E)|^2$. This simply reflects the fact that the pole position of the Z_b lies on

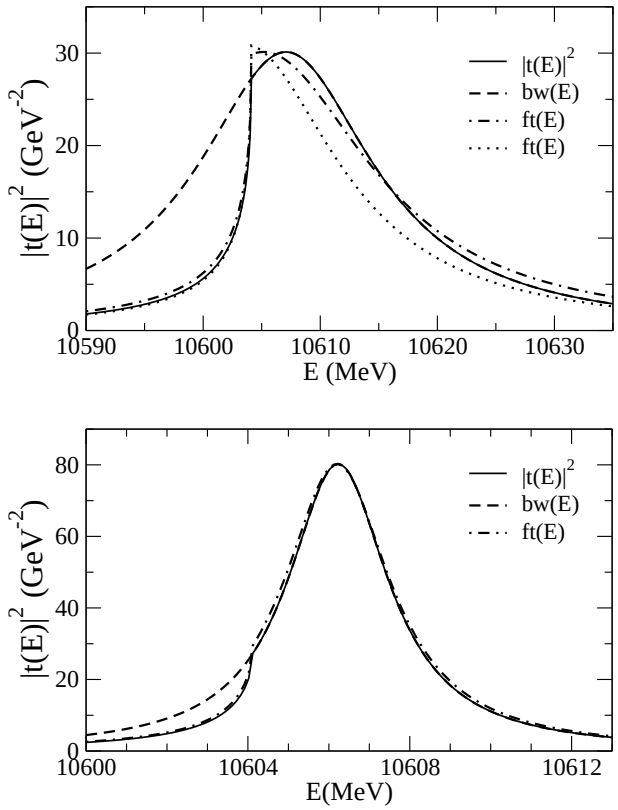

FIG. 1. Amplitude squared for uncoupled isovector S-wave $B\overline{B}^*$ scattering: $|t(E)|^2$ with $t(E)$ given by the ERE (solid line), Eq. (5); the Breit Wigner function $bw(E)$ (dashed line), Eq. (76); the Flatté parameterization $ft(E)$ (dash-dotted line), Eq. (77). The dotted line in the top panel corresponds to a Flatté parameterization in which $M'_R = M_{\rm th} + \frac{|k_R|^2}{2\mu}$, cf. Eq. (81).

the 2nd RS, and this RS connects continuously with the physical energy axis only above the $B\overline{B}^*$ threshold.[8] Below this threshold the form of the rise is a typical cusp effect which is enhanced because the pole of the Z_b fixes the size of $t(E)$ at the threshold point. On the other hand, we observe that the Flatté parameterization $ft(E)$ can reproduce accurately the cusp effect for $E < M_{\rm th}$, while it agrees worse with $|t(E)|^2$ than the Breit-Wigner function for $E > M_{\rm th}$. The Flatté parameterization as a function of energy shows above threshold a different qualitative form compared with $|t(E)|^2$, although they are not very different quantitatively.

The reason for this disagreement above threshold lies in the fact that Γ_R is significantly larger than $M_R - M_{\rm th}$ and this softens the energy dependence of $|t(E)|^2$ around the $B\overline{B}^*$ threshold compared with the abrupter effects implied by Eq. (78) when implemented in Eq. (77).[9] According to the previous discussion, in order to end with a situation in which the Flatté parameterization matches $|t(E)|^2$ above threshold, we decrease the width of the pole obtained from the ERE approximation by decreasing r and keeping a fixed (so that X decreases). If we take $r = -5.5$ fm the pole position is now $(10606.2 - i3.0)$ MeV (with $X = 0.32$); the width is six times smaller, while the resonance mass changes very little. Since now the imaginary part of the pole position has a size comparable with $M_R - M_{\rm th} \simeq 2$ MeV we should then expect a better agreement with the Flatté distribution. This is indeed what happens as plotted in the bottom panel of Fig. 1, where the Flatté distribution is able to reproduce faithfully $|t(E)|^2$ in the whole energy range shown. Once more, the Breit-Wigner parameterization with constant width perfectly matches $|t(E)|^2$ above threshold.

We can indeed rewrite Eq. (5) by taking into account the presence of the resonance, so that Eq. (16) is fulfilled. Equation (5) then becomes

$$t(E) = \frac{1}{(\frac{r}{2}(k - k_R) - i)(k + k_R)} \tag{80}$$

$$= \frac{-k_i/\mu}{E - M_{\rm th} - \frac{|k_R|^2}{2\mu} + ikk_i/\mu} \, . \tag{81}$$

The difference with respect to the Flatté parameterization in Eq. (77) stems from the fact that now one has

$$\gamma(E) = -\frac{2\gamma_k^2 k k_r}{\mu} \tag{82}$$

instead of $\Gamma_R(E)$, with $|k_R|$ substituted by $-k_r$. Again in the limit of small width both expressions agree but for $\Gamma_R \gg |M_R - M_{\rm th}|$ they are markedly different, because in such a case $|k_R| \simeq -k_r\sqrt{2}$, cf. Eq. (35), and then $\Gamma_R(E) \simeq \gamma(E)\sqrt{2}$. Due also to this reason, if we directly identify M'_R with $M_{\rm th} + \frac{|k_R|^2}{2\mu}$ in $ft(E)$, as read from Eq. (81), we obtain different results, corresponding to the dotted line in the top panel of Fig. 1. The disagreement between $ft(E)$ and $|t(E)|^2$ in this case is quite worse than the one between the solid and dash-dotted lines in the top panel of Fig. 1. The adjusting process for M'_R, Eq. (79), reduces the differences. In conclusion, for the case of the $Z_b^{(\prime)}$ resonances the use of Breit-Wigner functions to fit data [9–11] seems to be a reasonable approach, as long as the resonance mass is clearly above threshold. This conclusion is reflected by similarity between the solid and dashed lines in Fig. 1. Indeed, the peak position fixes the Breit-Wigner mass in $bw(E)$ in a precise way (in agreement with M_R), while one could certainly obtain

[8] The overlapping between different RS's is discussed in detail in Ref. [66].

[9] Notice that in the Laurent series around the pole position of the resonance the function $t(E)$ and its derivatives are evaluated at $E_R = M_R - i\Gamma_R/2$. This is why for $\Gamma_R \gg |M_R - M_{\rm th}|$ the effects of the branch point for $M_R \simeq M_{\rm th}$ are softened.

a reasonable estimate for the width by comparing $|t(E)|^2$ and the approximate $bw(E)$ curve. Nonetheless, sounder theoretical parameterizations of data should be pursued so as to pin down resonance parameters more accurately. In this respect, the modified version of the Flatté parameterization corresponding to Eq. (81), exactly reproduces $|t(E)|^2$ from the ERE.

V. SUMMARY AND CONCLUSIONS

In this work we study the resonances $Z_b(10610)$ (Z_b) and $Z_b(10650)$ (Z_b') based on analyticity and unitarity as basic principles of scattering theory. The dynamics is encoded in the pole positions of the resonances, which allows us to determine from unitarity the couplings of these resonances to $B\overline{B}^*$ and $B^*\overline{B}^*$, in order. These basic principles also determine the compositeness coefficient (X) of a resonance into an open two-body channel, as shown in Ref. [45]. We adapt these results to nonrelativistic scattering and obtain that X can be calculated for resonances whose mass is larger than threshold. By employing the uncoupled effective range expansion (ERE), up to including $\mathcal{O}(k^2)$ terms, X can be directly expressed in terms of the measurable scattering length (a) and effective range (r) as $X = 1/\sqrt{2r/a-1}$. With $k_R = k_r + ik_i$ ($k_i > 0, k_r < 0$), the two-body three-momentum at the resonance pole position, one can also express X in terms of the resonance mass M_R and width Γ_R as $X = -k_i/k_r$. For a small ratio $2|M_R - M_{\rm th}|/\Gamma_R$ this expression simplifies to $X = 1 - 2|M_R - M_{\rm th}|/\Gamma_R + \mathcal{O}((|M_R - M_{\rm th}|/\Gamma_R)^2)$, being $M_{\rm th}$ the threshold energy.

We first perform an ERE study of uncoupled isovector S-wave $B^{(*)}\overline{B}^*$ scattering, because it has the same quantum numbers as $Z_b^{(\prime)}$ [9] and these resonances lie in the vicinity of the open-bottom meson thresholds. It is then worth first focusing just on S-wave. Nevertheless, the associated three-momentum at the resonance pole position (k_R) has a modulus around m_π, with m_π the pion mass. In connection with this, we argue that although the branch point due to one pion exchange (at $k = im_\pi/2$) could severely restrict the applicability of ERE to $B^{(*)}\overline{B}^*$ scattering up to the resonance pole positions, this seems not finally be the case because of the perturbative nature of pions in the present systems. Namely, we consider estimates based on power counting in effective field theory [39] which shows that the iteration of pion exchanges is suppressed by a large expansion scale Λ for the isovector $B^{(*)}\overline{B}^*$ systems ($\Lambda \gg m_\pi$). This suppression is in line with the observation of Ref. [26], also reflected in specific calculations [15, 26, 40], that the exchanges of light $q\bar{q}$ mesons are OZI suppressed for the isovector $B^{(*)}\overline{B}^*$ scattering. The very same power counting study of Ref. [39] also establishes that coupling effects between different channels should be suppressed, at least a next-to-leading effect. This also matches with the experimental large branching ratios of the $Z_b^{(\prime)}$ into $B^{(*)}\overline{B}^*$, measured in Ref. [10]. As a result, the ERE study of the uncoupled isovector S-wave $B^{(*)}\overline{B}^*$ scattering seems an adequate first approximation to the problem.

Within this working assumption, we apply the ERE up to including $\mathcal{O}(k^2)$ and the real parameters involved, a and r, are fixed so as to reproduce the pole positions of the $Z_b^{(\prime)}$ resonances according to their masses and widths. The resulting values of a and $r \sim -(1-2)$ fm for both resonances have a size of around the standard range of strong interactions. This in turn indicates that the $B^{(*)}\overline{B}^*$ scattering near threshold would rather correspond to a potential scattering problem, which also implies that other compact components in the $Z_b^{(\prime)}$ states would play a relatively minor role. This is based on the observation that otherwise the nearby presence of a CDD pole would imply large contributions to $|r|$, cf. Eq. (8). Note that a priori, within an uncoupled S-wave ERE for $B^{(*)}\overline{B}^*$ scattering, the magnitude of the effective range r could be very different compared to the standard potential scattering problem. See Ref. [42] for a concrete example of a physical system with a resonance on top of thresholds that requires large values for $|r|$ and small ones of X.

This conclusion on the inner structure of the $Z_b^{(\prime)}$ states is further supported through the quantitative calculation of the compositeness X within ERE. We find that $X = 1/\sqrt{2r/a-1}$ and obtain the numerical values $X = 0.75 \pm 0.15$ and 0.67 ± 0.16 for the Z_b and Z_b', in order. These numbers are rather close to 1, which occurs whenever $\Gamma_R \gg M_R - M_{\rm th}$ ($M_R \geq M_{\rm th}$). This is a qualitative feature realized in many XYZ resonances and that indicates that the corresponding states would have an important two-heavy-particle component in their compositeness (as long as the application of uncoupled ERE is justified). We also derive a scaling law for the width of purely composite two-heavy-particle resonances in S-wave such that $\Gamma \sim 2\Lambda_{\rm QCD}^2/\mu \gg M_R - M_{\rm th}$, where $\Lambda_{\rm QCD} \simeq 200$ MeV, μ is the reduced mass of the two-heavy particles.

In the last part of the paper, we apply the method of Ref. [1] that only relies on the expressions for compositeness and the partial decay width of a resonance (taking into account its mass distribution). In particular, its applicability is not directly affected neither by nearby branch points from crossed-particle exchanges nor by the presence of other channels. Although, in connection with this, the validity of the Lorentzian mass distribution for the resonance is assumed to hold. In this way we can take into account the fact that the branching ratios of $Z_b^{(\prime)}$ to $B^{(*)}\overline{B}^*$, although rather large, are less than 1. After showing that consistent results with the ERE study are obtained under the same basic assumption (that the total width of the resonance is saturated by its partial decay width into $B^{(*)}\overline{B}^*$), we apply the method of Ref. [1] to find the actual value of compositeness ($X_{\rm ex}$). We finally obtain that $X_{\rm ex} = 0.66 \pm 0.11$ and $X_{\rm ex} = 0.51 \pm 0.10$ for the Z_b and Z_b', respectively, in accordance with the

experimentally measured branching ratios. The $B^{(*)}\overline{B}^{*}$ components found indicate that the $B\overline{B}^{*}$ is dominant among the components of the Z_b, but around half of the composition for the Z_b'. Other contributions then also play an important role in the inner composition of these resonances (particularly for the latter).

We also perform a comparison between the ERE approximation for the isovector S-wave $B^{(*)}\overline{B}^{*}$ scattering amplitude squared, $|t(E)|^2$, and the Breit-Wigner and Flatté parameterizations. This comparison could shed light on the issue of whether it is appropriate to apply Breit-Wigner functions to fit data in the experimental study of the $Z_b^{(\prime)}$ resonances. The reason is because the applicability of the ERE is not affected by the nearby $B^{(*)}\overline{B}^{*}$ threshold, while this is the case for both Breit-Wigner and Flatté parameterizations. We obtain that there is a marked cusp effect for energies below threshold that can be well reproduced by a Flatté parameterization. However, the use of the Breit-Wigner function with constant width for resonance peaks above threshold accurately reproduces $|t(E)|^2$ for $E > M_{\rm th}$ (including the maximum of the amplitude squared which fixes the resonance mass). We have also derived a variant of Flatté parameterization that exactly reproduces $|t(E)|^2$ from ERE. All in all, we conclude that it seems plausible to use Breit-Wigner functions to study the $Z_b^{(\prime)}$, though sounder parameterizations are clearly required to improve accuracy.

Needless to say that the method developed in Refs. [1, 42] and in this work, employed here to study the $Z_b^{(\prime)}$ resonances, could be also applied to other near-threshold resonances, and work along this direction is ongoing.

ACKNOWLEDGEMENTS

J.A.O. would like to thank David Rodríguez Entem for discussions on the sign of the ERE parameters and local interactions. This work is supported in part by the MINECO (Spain) and ERDF (European Commission) grant FPA2013-40483-P and the Spanish Excellence Network on Hadronic Physics FIS2014-57026-REDT, the National Natural Science Foundation of China (NSFC) under Grant Nos. 11575052 and 11105038, the Natural Science Foundation of Hebei Province with contract No. A2015205205, the grants from the Education Department of Hebei Province under contract No. YQ2014034, the grants from the Department of Human Resources and Social Security of Hebei Province with contract No. C201400323, the Sino-German Collaborative Research Center "Symmetries and the Emergence of Structure in QCD" (CRC 110) co-funded by the DFG and the NSFC.

[1] U. G. Meißner and J. A. Oller, Phys. Lett. B **751** (2015) 59.
[2] S. K. Choi *et al.* [Belle Collaboration], Phys. Rev. Lett. **91**, 262001 (2003) [hep-ex/0309032].
[3] K. A. Olive *et al.* [Particle Data Group Collaboration], Chin. Phys. C **38**, 090001 (2014).
[4] X. Liu, Chin. Sci. Bull. **59**, 3815 (2014) [arXiv:1312.7408 [hep-ph]].
[5] S. L. Olsen, PoS Bormio 050 (2015) [arXiv:1511.01589 [hep-ex]].
[6] H. X. Chen, W. Chen, X. Liu and S. L. Zhu, arXiv:1601.02092 [hep-ph].
[7] H. A. Bethe, Phys. Rev. **76** (1949) 38.
[8] M. A. Preston and B. K. Bhaduri, *Structure of the nucleus* (Addison-Wesley Publishing Company, Inc., Massachusetts, 1975).
[9] A. Bondar *et al.* [Belle Collaboration], Phys. Rev. Lett. **108**, 122001 (2012) [arXiv:1110.2251 [hep-ex]].
[10] I. Adachi *et al.* [Belle Collaboration], arXiv:1209.6450 [hep-ex].
[11] I. Adachi [Belle Collaboration], arXiv:1105.4583 [hep-ex].
[12] A. Garmash *et al.* [Belle Collaboration], Phys. Rev. D **91**, no. 7, 072003 (2015) [arXiv:1403.0992 [hep-ex]].
[13] D. V. Bugg, Europhys. Lett. **96**, 11002 (2011) [arXiv:1105.5492 [hep-ph]]; Phys. Lett. B **598**, 8 (2004) [hep-ph/0406293].
[14] E. S. Swanson, Phys. Rev. D **91**, no. 3, 034009 (2015) [arXiv:1409.3291 [hep-ph]].
[15] D. Y. Chen and X. Liu, Phys. Rev. D **84**, 094003 (2011) [arXiv:1106.3798 [hep-ph]].
[16] F. K. Guo, C. Hanhart, Q. Wang and Q. Zhao, Phys. Rev. D **91**, no. 5, 051504 (2015) [arXiv:1411.5584 [hep-ph]].
[17] A. E. Bondar, A. Garmash, A. I. Milstein, R. Mizuk and M. B. Voloshin, Phys. Rev. D **84**, 054010 (2011) [arXiv:1105.4473 [hep-ph]]; *ibid.* **84**, 031502 (2011) [arXiv:1105.5829 [hep-ph]]. X. Li and M. B. Voloshin, *ibid.* **86**, 077502 (2012) [arXiv:1207.2425 [hep-ph]]
[18] M. Cleven, F. K. Guo, C. Hanhart and U. G. Meißner, Eur. Phys. J. A **47**, 120 (2011) [arXiv:1107.0254 [hep-ph]].
[19] M. Cleven, Q. Wang, F. K. Guo, C. Hanhart, U. G. Meißner and Q. Zhao, Phys. Rev. D **87**, no. 7, 074006 (2013) [arXiv:1301.6461 [hep-ph]].
[20] J. Nieves and M. P. Valderrama, Phys. Rev. D **84**, 056015 (2011) [arXiv:1106.0600 [hep-ph]].
[21] F. K. Guo, C. Hidalgo-Duque, J. Nieves and M. P. Valderrama, Phys. Rev. D **88**, 054007 (2013) [arXiv:1303.6608 [hep-ph]].
[22] Y. Yang, J. Ping, C. Deng and H. S. Zong, J. Phys. G **39**, 105001 (2012) [arXiv:1105.5935 [hep-ph]]; M. T. Li, W. L. Wang, Y. B. Dong and Z. Y. Zhang, *ibid.* **40**, 015003 (2013) [arXiv:1204.3959 [hep-ph]].
[23] Z. F. Sun, J. He, X. Liu, Z. G. Luo and S. L. Zhu, Phys. Rev. D **84**, 054002 (2011) [arXiv:1106.2968 [hep-ph]];
[24] X. H. Liu, L. Ma, L. P. Sun, X. Liu and S. L. Zhu, Phys. Rev. D **90**, no. 7, 074020 (2014) [arXiv:1407.3684 [hep-

ph]].
[25] Y. Dong, A. Faessler, T. Gutsche and V. E. Lyubovitskij, J. Phys. G **40**, 015002 (2013) [arXiv:1203.1894 [hep-ph]].
[26] J. M. Dias, F. Aceti and E. Oset, Phys. Rev. D **91**, no. 7, 076001 (2015) [arXiv:1410.1785 [hep-ph]].
[27] T. Mehen and J. W. Powell, Phys. Rev. D **84**, 114013 (2011) [arXiv:1109.3479 [hep-ph]]; *ibid.* **88**, no. 3, 034017 (2013) [arXiv:1306.5459 [hep-ph]].
[28] S. Ohkoda, Y. Yamaguchi, S. Yasui, K. Sudoh and A. Hosaka, Phys. Rev. D **86**, 014004 (2012) [arXiv:1111.2921 [hep-ph]].
[29] A. Ali, C. Hambrock and W. Wang, Phys. Rev. D **85**, 054011 (2012) [arXiv:1110.1333 [hep-ph]]; A. Ali, L. Maiani, A. D. Polosa and V. Riquer, Phys. Rev. D **91**, no. 1, 017502 (2015) [arXiv:1412.2049 [hep-ph]].
[30] E. Braaten, C. Langmack and D. H. Smith, Phys. Rev. D **90**, no. 1, 014044 (2014) [arXiv:1402.0438 [hep-ph]].
[31] S. Dubynskiy and M. B. Voloshin, Phys. Lett. B **666**, 344 (2008) [arXiv:0803.2224 [hep-ph]].
[32] I. V. Danilkin, V. D. Orlovsky and Y. A. Simonov, Phys. Rev. D **85**, 034012 (2012) [arXiv:1106.1552 [hep-ph]].
[33] J. R. Zhang, M. Zhong and M. Q. Huang, Phys. Lett. B **704**, 312 (2011) [arXiv:1105.5472 [hep-ph]];
[34] Z. G. Wang and T. Huang, Eur. Phys. J. C **74**, no. 5, 2891 (2014) [arXiv:1312.7489 [hep-ph]]; Z. G. Wang, Eur. Phys. J. C **74**, no. 7, 2963 (2014), [arXiv:1403.0810 [hep-ph]].
[35] F. S. Navarra, M. Nielsen and J. M. Richard, J. Phys. Conf. Ser. **348**, 012007 (2012) [arXiv:1108.1230 [hep-ph]].
[36] C. Y. Cui, Y. L. Liu and M. Q. Huang, Phys. Rev. D **85**, 074014 (2012) [arXiv:1107.1343 [hep-ph]].
[37] Z. G. Wang and T. Huang, Nucl. Phys. A **930**, 63 (2014) [arXiv:1312.2652 [hep-ph]].
[38] J. Segovia, P. G. Ortega, D. R. Entem and F. Fernndez, arXiv:1601.05093 [hep-ph]. This reference employs the constituent quark model of J. Vijande, F. Fernandez and A. Valcarce, J. Phys. G **31**, 481 (2005) [hep-ph/0411299].
[39] M. P. Valderrama, Phys. Rev. D **85**, 114037 (2012) [arXiv:1204.2400 [hep-ph]].
[40] H. W. Ke, X. Q. Li, Y. L. Shi, G. L. Wang and X. H. Yuan, JHEP **1204**, 056 (2012) [arXiv:1202.2178 [hep-ph]].
[41] X. W. Kang, J. Haidenbauer and U. G. Meißner, JHEP **1402**, 113 (2014) [arXiv:1311.1658 [hep-ph]]; Nucl. Phys. A **929**, 102 (2014) [arXiv:1405.1628 [nucl-th]]; Phys. Rev. D **91**, no. 7, 074003 (2015) [arXiv:1502.00880 [nucl-th]]; Phys. Rev. D **92**, no. 5, 054032 (2015) arXiv:1506.08120 [nucl-th].
[42] Z. H. Guo and J. A. Oller, Phys. Rev. D **93**, 054014 (2016) arXiv:1601.00862[hep-ph].
[43] T. Hyodo, Phys. Rev. Lett. **111**, 132002 (2013) [arXiv:1305.1999 [hep-ph]].
[44] W. S. Huo and G. Y. Chen, arXiv:1501.02189 [hep-ph].
[45] Z. H. Guo and J. A. Oller, arXiv:1508.06400 [hep-ph].
[46] S. Fleming, M. Kusunoki, T. Mehen and U. van Kolck, Phys. Rev. D **76**, 034006 (2007) [hep-ph/0703168].
[47] D. B. Kaplan, M. J. Savage and M. B. Wise, Phys. Lett. B **424**, 390 (1998) [nucl-th/9801034] ; Nucl. Phys. B **534**, 329 (1998) [nucl-th/9802075].
[48] F. Aceti, M. Bayar, E. Oset, A. Martinez Torres, K. P. Khemchandani, J. M. Dias, F. S. Navarra and M. Nielsen, Phys. Rev. D **90**, no. 1, 016003 (2014) [arXiv:1401.8216 [hep-ph]]; F. Aceti, M. Bayar, J. M. Dias and E. Oset, Eur. Phys. J. A **50**, 103 (2014) [arXiv:1401.2076 [hep-ph]].
[49] J. A. Oller and E. Oset, Phys. Rev. D **60** (1999) 074023.
[50] G. F. Chew and S. Mandelstam, Phys. Rev. **119**, 467 (1960).
[51] S. Weinberg, Phys. Rev. **130** (1963) 776.
[52] V. Baru, J. Haidenbauer, C. Hanhart, Y. Kalashnikova and A. E. Kudryavtsev, Phys. Lett. B **586** (2004) 53.
[53] T. Hyodo, D. Jido and A. Hosaka, Phys. Rev. C **85** (2012) 015201.
[54] F. Aceti and E. Oset, Phys. Rev. D **86** (2012) 014012.
[55] T. Sekihara, T. Hyodo and D. Jido, PTEP **2015** 6, 063D04 [arXiv:1411.2308 [hep-ph]].
[56] D. Agadjanov, F.-K. Guo, G. Rios and A. Rusetsky, JHEP **1501** (2015) 118 [arXiv:1411.1859 [hep-lat]].
[57] U. van Kolck, Nucl. Phys. A **645**, 273 (1999) [nucl-th/9808007].
[58] D. R. Phillips and T. D. Cohen, Phys. Lett. B **390**, 7 (1997) doi:10.1016/S0370-2693(96)01411-6 [nucl-th/9607048].
[59] H. T. C. Stoof, K. B. Gubbels and D. B. M. Dickerscheid, *Ultracold Quantum Fields* (Springer, Dordrecht, 2009). Chapter 10.
[60] H. M. Nussenzveig, Nucl. Phys. **11**, 499 (1959).
[61] J. A. Oller and E. Oset, Nucl. Phys. A **620**, 438 (1997) [Nucl. Phys. A **652**, 407 (1999)] [hep-ph/9702314].
[62] R. Aaij *et al.* [LHCb Collaboration], Phys. Rev. Lett. **115**, 072001 (2015) [arXiv:1507.03414 [hep-ex]].
[63] Y. H. Chen, J. T. Daub, F. K. Guo, B. Kubis, U. G. Meißner and B. S. Zou, Phys. Rev. D **93**, no. 3, 034030 (2016) doi:10.1103/PhysRevD.93.034030 [arXiv:1512.03583 [hep-ph]].
[64] C. Hanhart, Y. S. Kalashnikova, P. Matuschek, R. V. Mizuk, A. V. Nefediev and Q. Wang, Phys. Rev. Lett. **115**, no. 20, 202001 (2015) [arXiv:1507.00382 [hep-ph]].
[65] S. M. Flatté, Phys. Lett. B **63**, 224 (1976).
[66] J. A. Oller, Eur. Phys. J. A **28**, 63 (2006) [hep-ph/0603134].